



# Antibacterial, Antifungal, and Antitumor Properties of 2,5-Pyrrolidinedione Derivatives

Sultan D. Y. Albakhit<sup>1,2</sup> · Dakhil Zughayir Mutlaq<sup>1</sup> · Ali A. A. Al-Shawi<sup>1</sup>

Received: 12 April 2023 / Accepted: 21 May 2023  
© The Tunisian Chemical Society and Springer Nature Switzerland AG 2023

## Abstract

Succinimide and maleimide reactions were used to create analogues of novel twelve derivatives (**5a–5l**). The compounds contain a variety of functional groups, including Br, Cl, CH<sub>3</sub>, OH, and OCH<sub>3</sub>. The <sup>1</sup>H-NMR, <sup>13</sup>C-NMR, FT-IR, and mass spectra were used to characterize the new compounds. These new compounds were studied for their antimicrobial and anticancer properties. MIC values for antibacterial and antifungal activities were determined. The results showed that compounds **5a**, **5b**, **5c**, **5g**, **5h**, **5k**, and **5l** have good MIC values (0.25, 0.5, 0.5, 0.25, 0.5, 0.5, and 0.5 μM, respectively) against gram positive *Enterococcus faecalis*, while compounds **5a**, **5b**, **5c**, **5d**, **5e**, **5g**, **5h**, **5j**, and **5k** have MIC values (0.125, 0.5, 0.5, 0.25, 0.25, 0.25, 0.5, 0.5 and 0.5 μM, respectively) against the fungal *C. albicans*. MCF7 cells were used for anticancer activity, and IC<sub>50</sub> values were calculated using the MTT assay. Compounds **5i** and **5l** have the highest potential activity against MCF-7, with IC<sub>50</sub> values of 1.496 and 1.831 μM, respectively. EB/AO staining, apoptosis, and reactive oxygen species experiments were used to evaluate the efficiency of IC<sub>50</sub> values of compounds **5i** and **5l**. The results revealed that both compounds have potential anticancer activity against MCF-7 cells. The results of compounds as antimicrobial (**5a** and **5g**) and anticancer (**5i** and **5l**) activities suggested that these compounds, particularly could be developed as potential drugs in the future. Merit investigations seek to comprehend the action mechanism.

**Keywords** Succinimide derivatives · Antimicrobial · Maleimide derivatives · Breast cancer

## 1 Introduction

The succinimides are a fascinating class of heterocyclic compounds with widespread applications in chemical synthesis and biochemistry (pyrrolidine-2,5-diones). Succinimide compounds, for example, have anticonvulsant, anti-inflammatory, antitumor, and antimicrobial properties, as well as 5-HT receptor ligands and enzyme inhibitors. Simultaneously, SAR (Structure–Activity Relationship) analysis has gradually been acquired, and a large number

of derivatives for potential targets have been derived [1, 2]. As a result, novel succinimide compounds synthesized via synthetic methods are extremely appealing. One of the processes that results in substituted succinimide derivatives is the addition of nucleophiles to the double bond of maleimide via the Michael reaction [3].

Michael acceptors (aliphatic or aromatic amines, amides, carbamates, or azides) interact with Michael donors (vinyl ketones, vinyl sulfones, acrylamides, acrylonitrile, and vinylphosphonates) [4]. Maleimide derivatives are frequently used in bioconjugation procedures due to their high reactivity with thiols. Other hetero-Michael additions that maleimides can undergo include the less well-known aza-, phospho-, and oxa-Michael reactions [5].

Maleimides have been extensively studied in such reactions because, due to the presence of an activated double bond, they can be easily converted to substituted succinimides [6]. The succinimide molecule is used as a precursor in many important medications, including phen-suximide, ethosuximide, methsuximide, and andrimias [7, 8]. Analgesic [9], anticancer [10], antiparasitic

✉ Ali A. A. Al-Shawi  
ali.abdulhussein@uobasrah.edu.iq

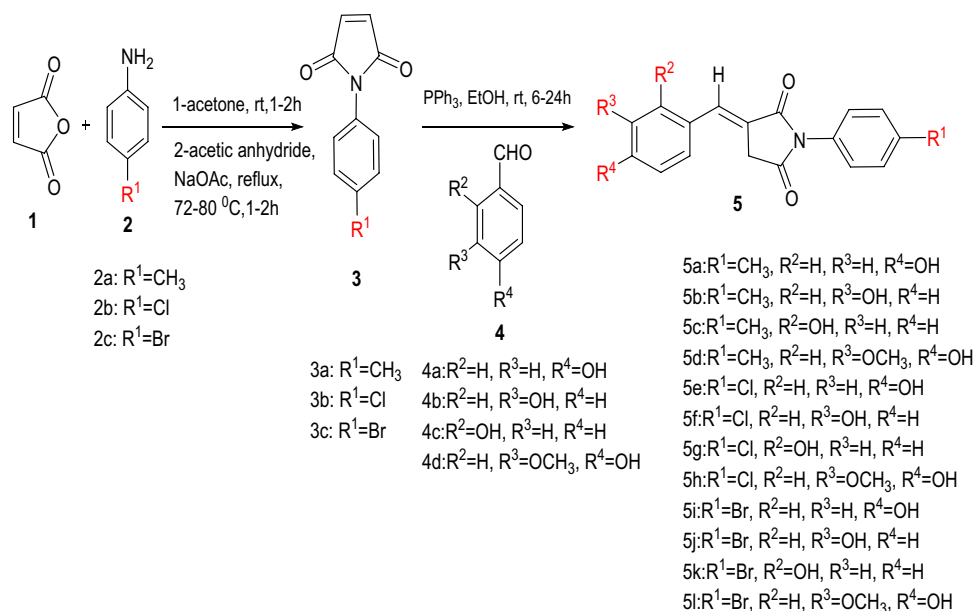
Sultan D. Y. Albakhit  
ceps213p0004@avicenna.uobasrah.edu.iq

Dakhil Zughayir Mutlaq  
dakhil.mutlaq@uobasrah.edu.iq

<sup>1</sup> Department of Chemistry, College of Education for Pure Sciences, University of Basrah, Basrah, Iraq

<sup>2</sup> Branch of Basic Sciences, College of Dentistry, University of Basrah, Basrah, Iraq

**Scheme 1** Represent the synthesis method of new series of succinimide derivatives (**5a–l**)



[11], antibiotic [12], and muscle relaxant [13] are a few examples.

The structure activity of succinimide revealed that phenyl substitution makes them active against electrically induced convulsion. N-methylation reduces resistance to electroshock seizures. N-methylation also improves resistance to chemically induced convulsions [14]. These properties of succinimide allow for the synthesis of potential derivatives in a variety of biological and pharmaceutical activity [15]. Previous structure activity studies demonstrated that succinimide-maleimide can be used for future derivative proposition, increasing the chances of obtaining potentially compounds with diverse biological applications [16, 17].

Breast cancer is the most common cancer in Iraq and the leading cause of death in women over the age of 50, it is ranked first among Iraq's top ten cancers. Environmental and food pollution, for example, contribute to an increase in cases each year [18]. According to World Health Organization statistics, males (14,070 new cases and 9,418 cancer deaths) will have a lower incidence of breast cancer in 2020 than females (19,803 new cancer cases and 10,368 cancer deaths) [19]. As a result, using medicinal chemistry to design and discover new small molecules as anti-breast cancer agents will improve chemotherapy treatment and reducing side effects, which are the main issues with chemotherapy treatment [20–23]. Our research focused on the synthesis of new series succinimide-maleimide derivatives with various functional groups in order to obtain more efficient compounds with antimicrobial and anti-breast cancer properties.

## 2 Results and Discussion

### 2.1 Chemistry

The creation of new derivatives with potential biological effects based on the use of substituent groups in maleimide and succinimide. The ortho, meta, and para positions of substituent groups (OH, OCH<sub>3</sub>, CH<sub>3</sub>, Cl, and Br) play a role in the expansion of biological functions. These variants were used to compare the synthesized compounds. Thus, we synthesized new analogues of succinimide-maleimide derivatives (**5a–l**).

First, maleamic acid derivatives were synthesized in an acetone solvent using maleic anhydride and amine. This intermediate was then cyclized in acetic anhydride in the presence of anhydrous sodium acetate to give the maleimide derivatives (**3a–c**) [24].

To avoid self-polymerization of the intermediate, the reaction rate and temperature were gradually increased in an ice bath by slowly adding substituted aniline. The intermediate was then converted to N-substituted maleimide via a condensation ring-closure reaction catalyzed by anhydrous sodium acetate in an acetic anhydride solvent. According to Kalia's method [25], triphenyl phosphine was gradually added to N-substituted maleimide (d), followed by the Wittig reaction with substituted benzaldehyde (**4a–d**), to yield the N-substituted-succinimide (**5a–l**) at room temperature, as showed in Scheme 1.

The FT-IR, <sup>1</sup>H-NMR, <sup>13</sup>C-NMR, and mass spectra were used to confirm the chemical structures of all of the resulting succinimide derivatives. The properties of the IR-absorption bands were determined using the KBr

disc (**5a–l**). The functional groups of these compounds were identified using the IR spectrum. The stretching bands associated with (OH) groups were observed in the 3419–3327  $\text{cm}^{-1}$  range. The absorption bands in the 1766–1691  $\text{cm}^{-1}$  range are associated with (C=O). The bands at 1649–1637  $\text{cm}^{-1}$  were caused by (C=C) aliphatic condensation.

The  $^1\text{H-NMR}$  spectra were generated using succinimide derivatives (**5a–l**). The solvents DMSO- $d_6$  and water are responsible for the signals at 2.5 and 3.3 ppm, respectively. Singlet signals ranging from 10.78 to 9.70 ppm were assigned to the OH. (C=CH) was responsible for the triplet signals ranging from 7.93 to 7.46 ppm. The protons of the  $\text{CH}_2$  were assigned doublet signals ranging from 3.83 to 3.76 ppm. At 7.75–6.88 ppm, aromatic protons were given the multiplet and doublet [26]. Singlets at 3.86–3.85 ppm were caused by the methoxy group, while singlets at 2.37–2.36 ppm were caused by the methyl group. Carbonyl groups were attributed to the  $^{13}\text{C-NMR}$  signals of compounds **5a–l** that ranged from 174.17 to 169.33 ppm. Carbon aromatic ring signals were detected in the range of 159.95–113.45 ppm, while aliphatic carbons were detected in the range of 56.10–21.23 ppm. The presence of a molecular ion ( $m/z$ ) was revealed in the mass spectra of the **5a–n** groups: 293.2 ( $\text{M}^+$ ), 293 ( $\text{M}^+$ ), 293 ( $\text{M}^+$ ), and 323 ( $\text{M}^+$ ), 313 ( $\text{M}^+$ ), 313 ( $\text{M}^+$ ), 343 ( $\text{M}^+$ ), 359 ( $\text{M}^+$ ), 357 ( $\text{M}^+$ ), 357 ( $\text{M}^+$ ), and 389 ( $\text{M}^+$ ). The mass spectra proved that the structures were correct.

## 2.2 Biological Activity Evaluation

### 2.2.1 Antimicrobial Activity

In our research, we synthesized twelve new compounds by reacting maleimide with various benzaldehydes featuring functional donating and withdrawing groups. These compounds were tested for antibacterial and antifungal properties and determined MIC values. As shown in Table 1, the compounds **5a**, **5b**, **5c**, **5g**, **5h**, **5k**, and **5l** have good MIC values (0.25, 0.5, 0.5, 0.25, 0.5, 0.5, and 0.5  $\mu\text{M}$ , respectively) against gram positive *E. faecalis*, while the compounds **5a**, **5b**, **5c**, **5d**, **5e**, **5g**, **5h**, **5i**, and **5k** have MIC values (0.125, 0.5, 0.5, 0.25, 0.25, 0.25, 0.5, 0.5, and 0.5  $\mu\text{M}$ , respectively) against the fungal *C. albicans*.

Because of the functional groups (**5a** has para-methyl and para-hydroxyl groups, **5g** has para-chloro and ortho-hydroxyl groups) that are donor and withdrawing groups. In addition, the hydroxyl group might play a role in the interaction with cell membrane via created hydrogen bonding with thiol group and leading to inhibit and break down the cells membrane, this mechanism could be understood and discussed in future research [27, 28]. Therefore, **5a** and **5g** showed a greater effect than the others against *E. faecalis*. Resistance to multiple antimicrobial drugs has rapidly increased over the last several decades, particularly among *E. faecalis*. Endocarditis, urinary tract infections, prostatitis, intra-abdominal infection, cellulitis, wound infection, and concurrent bacteremia are all caused by *E. faecalis* [29–31]. As a result, discovering new antimicrobial drugs will reduce bacterial infections and human risk. In terms of antifungal activity against *C. albicans*, **5a** has a lower MIC value than

**Table 1** Represent the antimicrobial activity of compounds (**5a–5l**) and their estimated MIC values using gram positive bacteria (*S. mutans*, *E. faecalis*, *S. aureus*) and gram negative bacteria (*E. Coli* and *P. aeruginosa*), and the fungal *C. albicans*

Compound symbol	Bacterial MIC ( $\mu\text{g/ml}$ )					Fungal MIC ( $\mu\text{g/ml}$ )
	Gram positive			Gram negative		
	<i>S. mutans</i>	<i>E. faecalis</i>	<i>S. aureus</i>	<i>E. coli</i>	<i>P. aeruginosa</i>	
<b>5a</b>	4	0.25	1	4	4	0.125
<b>5b</b>	2	0.5	2	4	4	0.5
<b>5c</b>	4	0.5	1	4	4	0.5
<b>5d</b>	4	1	1	4	4	0.25
<b>5e</b>	4	2	1	4	4	0.25
<b>5f</b>	4	2	2	4	2	1
<b>5g</b>	4	0.25	1	2	2	0.25
<b>5h</b>	<4	0.5	2	4	2	0.5
<b>5i</b>	4	1	1	2	2	1
<b>5j</b>	4	1	2	4	4	0.5
<b>5k</b>	4	0.5	2	2	2	0.5
<b>5l</b>	<4	0.5	4	4	2	2
Cefixime	0.1411	0.1411	0.0022	0.0002	0.2822	–
Cycloheximide	–	–	–	–	–	0.0035

others. This is because the donor group (CH<sub>3</sub>) has a para-hydroxyl group function. *C. albicans* is a fungus that lives in small amounts on human body, primarily in mouth, skin, and intestines. *Candida* is yeast that, when out of balance with healthy bacteria in the body, causes infections such as thrush and vaginal yeast infections. Infections are common and are treated with antifungal drugs. On the other hand, the donor and withdrawing groups in a compound may reduce its potential activity, so it was discovered that the donor group has a moderate effect than the withdrawing group for antimicrobial activities.

## 2.2.2 Anticancer Activity

### 2.2.2.1 MTT Assay and AO/EB Staining

Twelve succinimide derivatives were tested against breast cancer cells (MCF-7) in this study, and their IC<sub>50</sub> values are shown in Table 2. Among these compounds, **5i** and **5l** have lower IC<sub>50</sub> values (1.496 and 1.831 μM, respectively), compared with cisplatin IC<sub>50</sub> value (3.653 μM) as positive control drug.

This cytotoxicity could be caused by the activity of the functional groups. While **5i** contains bromide and *para*-hydroxyl groups, **5l** contains bromide, *meta*-methoxy, and *para*-hydroxyl groups. The withdrawing group (bromide in **5i** compound) increases compound potential activity, whereas the donor group (methoxy) and withdrawing group (bromide) in **5l** compound may decrease compound potential activity. Suggested that methoxy group might influence compound **5l** activity. The type of side chain substituent is also important in inducing cytotoxicity and apoptosis-signaling pathways. Lipophilicity is a critical physicochemical property that influences absorption, distribution, metabolism, excretion, and toxicity properties, as well as the overall suitability of drug candidates. Furthermore, highly lipophilic compounds have a tendency to bind to hydrophobic targets other than the desired target, increasing the risk of promiscuity and toxicity. When IC<sub>50</sub> values are compared, compounds with lower lipophilicity are less cytotoxic. Furthermore, we used EB/AO staining, apoptosis, and ROS experiments to determine the IC<sub>50</sub> values of compounds **5i** and **5l** to target their anticancer functions. Figure 1 depicted the impact of compounds **5i** and **5l** on cells viability staining and DNA fragmentation. The difference in dye permeability into the intact cell membrane is used to differentiate viable, apoptotic, and necrotic cells. Green cells are viable and stained only with AO; green and orange cells with condensed chromatin are early and late apoptotic cells, and are stained with both AO and EB (with a moderate change in membrane permeability); and necrotic cells are orange and stained with EB.

When compared to control cells, **5i** has a higher effect on cells. These findings suggest that the tests **5i** and **5l** may intercalate into DNA, potentially causing DNA damage.

Hereby, we used apoptosis analysis to improve the EB/AO staining results, as shown in Fig. 2, the late apoptosis ratio of MCF-7 cells treated with IC<sub>50</sub> value of **5i** (13.82%) was higher than **5l** (13.53%), compared to apoptosis of control cells (99.77%).

In addition, **5i** and **5l** were used to determine their effect on ROS production, and the Count-FL1 plot was used to interpret the ROS production. There is no significant peak in the control sample in the RN1 area of the plot, indicating that the fluorescent from produced DCF compound is very low, indicating that the level of intercellular ROS is negligible (6%). The peak is visible in **5i** treated cells in the RN1 area and shows that the ROS level has increased significantly in **5i** treated cells (42%), and in cells treated with **5l** the ROS level is significantly higher (77%), as shown in Fig. 3.

Succinimide's pharmacology potential and structural features led the way for extensive synthesis and exploration involving docking and dynamics investigations of succinimide derivatives. As a result of their skeleton structure, it exhibits biological activities by creating carbon- or nitrogen-substituted derivatives with diverse aryl or alkyl groups that might generate potential therapeutic molecules. Few studies have shown that succinimide derivatives are efficacious against a variety of cancer cells, including breast cancer cells (MCF-7 and MDA-MB23) [32, 40]. Thus, some reports showed inactive succinimide derivatives as antimicrobial [33, 34]. Based on their biological roles, succinimide compounds could be developed for pharmacological applications in collaboration with docking and dynamics investigations.

## 3 Conclusions

Succinimides are highly reactive because they contain both carbonyl and methylene groups. Succinimide derivatives are important compounds in the development of many drug candidates. In this study, the antimicrobial and anticancer activities of a series novel succinimide-maleimide derivatives containing donor and withdrawing (methyl, chloro, bromide, methoxy, and hydroxyl) groups were evaluated. Bioassay results showed that some compounds (**5a** and **5g**) had a potential antimicrobial activity against *Enterococcus faecalis* and *Candida albicans*. While compounds **5i** and **5l** have a potential activity against MCF-7 cancer cells. This demonstrates that using succinimide-maleimide as an active substance in the design and synthesis of its derivatives is an excellent strategy for discovering new bioactive molecules. Specifically, in the development of more potent, safer, and selective breast cancer therapy candidates. Therefore, merit investigations for compounds **5a**, **5g**, **5i**, and **5l** for antimicrobial and anticancer activities enhanced by molecular docking and dynamics studies are requested.

**Table 2** Represent the chemical structure of succinimide derivatives (**5a–5i**) and their estimated IC<sub>50</sub> values

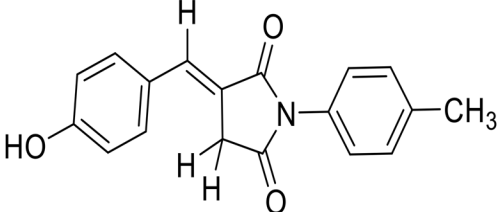
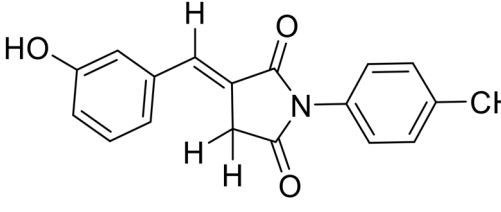
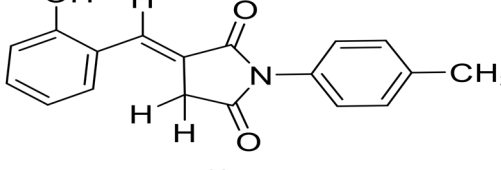
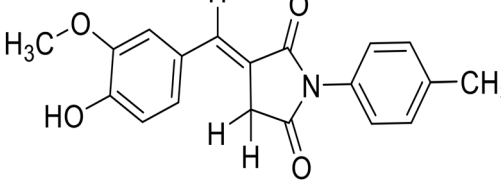
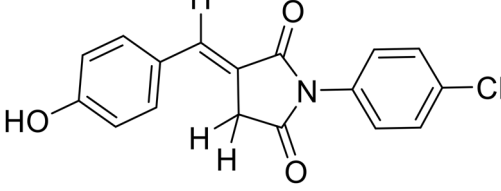
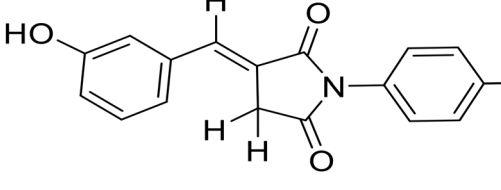
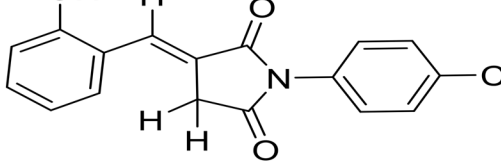
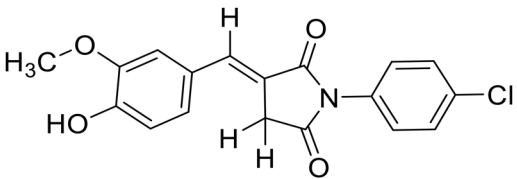
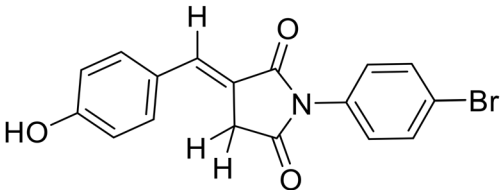
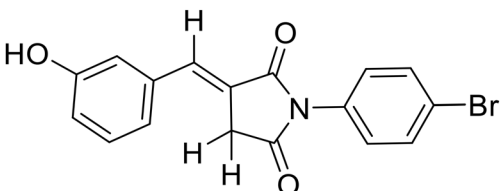
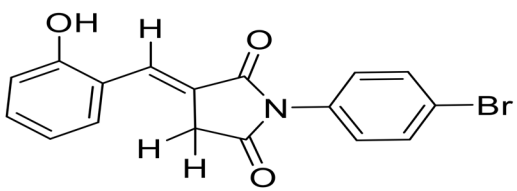
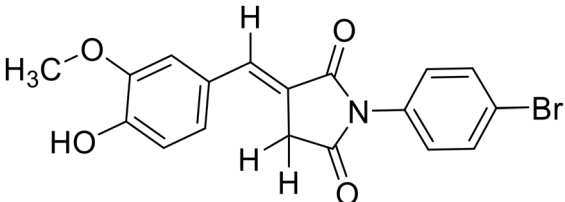
Symbol	Chemical structure	MCF-7 cells IC <sub>50</sub> in $\mu\text{M}$
5a		2.005
5b		2.111
5c		2.179
5d		3.189
5e		3.379
5f		2.087
5g		2.081

Table 2 (continued)

Symbol	Chemical structure	MCF-7 cells IC50 in $\mu\text{M}$
5h		1.895
5i		1.496
5j		2.128
5k		2.085
5l		1.831
Cis-platin (positive control)		3.653

## 4 Experimental

### 4.1 Chemistry Section

Sigma Aldrich supplied all of the chemical materials. Melting points were determined using a Gallenkamp melting point apparatus. Proton and carbon NMR spectra were recorded at 500 MHz and 125 MHz on the Bruker DRX 500 Advance spectrometer, respectively, using deuterated solvents and TMS as internal standard chemical shifts as ppm values. Perkin-Elmer FT-IR-1600 spectrophotometer was used to obtain infrared spectra. On aluminum sheets of Merck silica gel, thin-layer chromatography (TLC) was performed. The TLC spots were observed in UV and  $\text{I}_2$ . The mass spectrum was tested using the EI method at 70 eV with either the Agilent or Spectral technologies.

#### 4.1.1 Procedure for Synthesis Maleimides (3a–c)

Maleamic acid derivatives (0.02 mol) were dissolved in acetic anhydride (10 ml) and anhydrous sodium acetate (0.005 mol) was added, then the solution was cooled and poured into an ice bath with vigorous stirring, as described in the literature [35]. Using an appropriate solvent, the maleimide was precipitated, filtered, dried, and recrystallized.

#### 4.1.2 General Procedure the Synthesis of Compounds (5a–5l)

Dissolve (0.012 mol) of substituted maleimide in 30 ml of ethanol using a magnetic stirrer. After complete dissolution, 0.01 mol of triphenyl phosphine was slowly added for 4 to 5 min. Then (0.01 mol) ortho, meta, or

**Fig. 1** EB/AO staining assay showed: **A** untreated cells. **B** Cells treated with compound **5i**. **C** Cells treated with compound **5l**. Green cells are viable and stained only with AO; green and orange cells with condensed chromatin are early and late apoptotic cells, and are stained with both AO and EB; and necrotic cells are orange and stained with EB

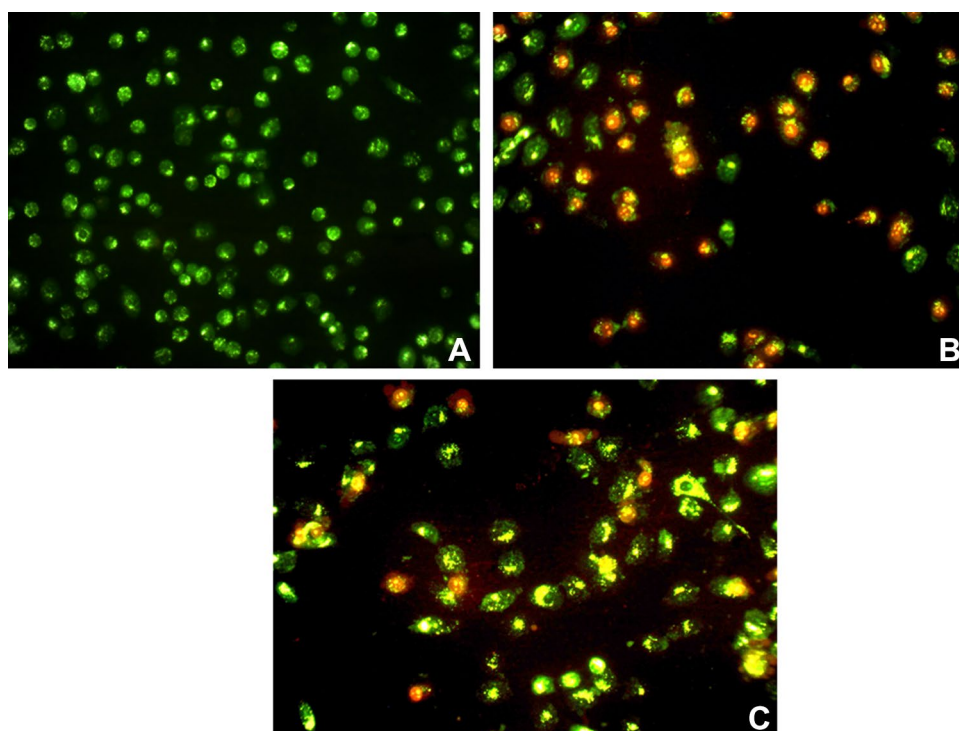
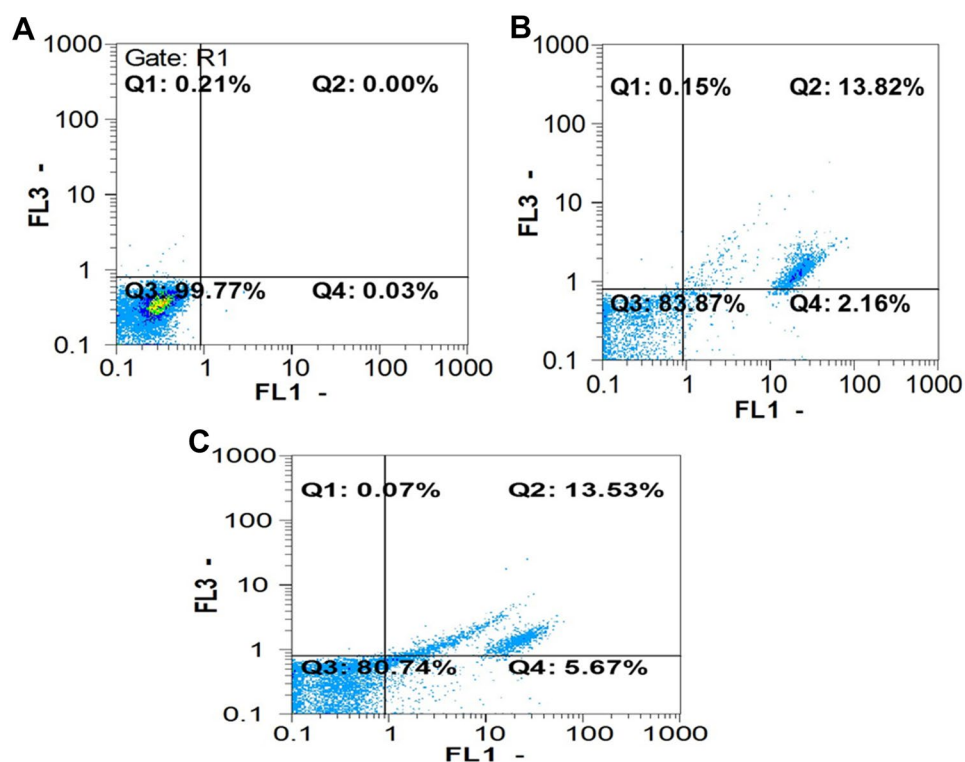


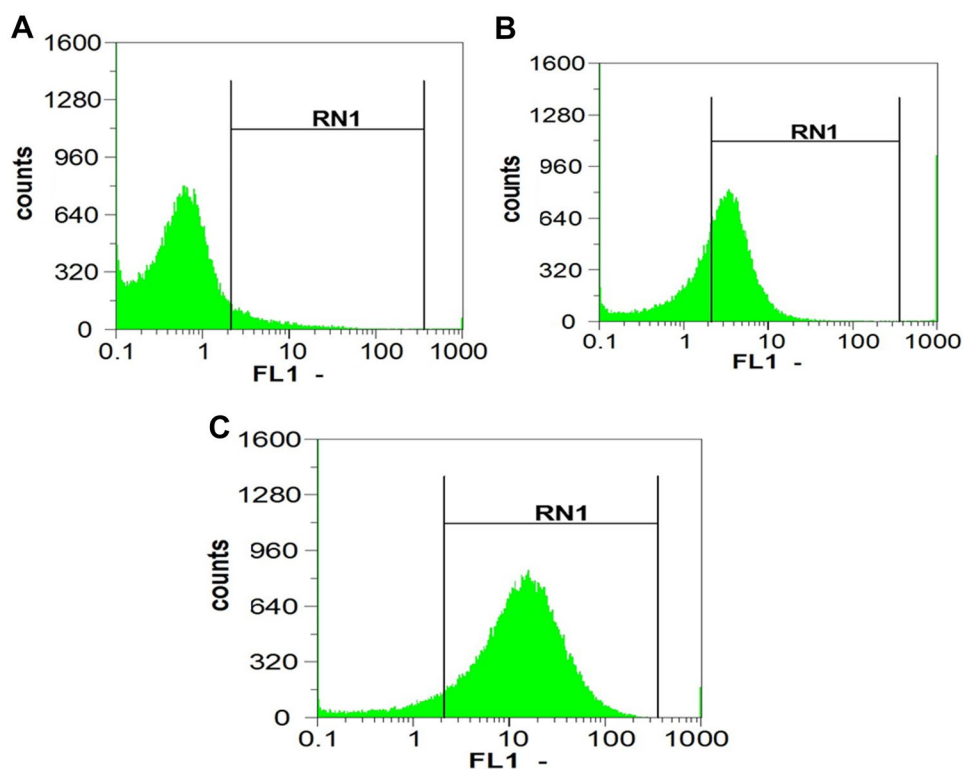
**Fig. 2** Apoptosis analysis using flowcytometry technique showed: **A** untreated cells. **B** Cells treated with compound **5i**. **C** Cells treated with compound **5l**



para-hydroxy benzaldehyde was quickly added, and after an hour of reaction, a white suspension was observed. For 24 h, the reaction was stirred at room temperature. TLC was used to monitor the completion of the reaction

process. Filtration was used to collect the precipitate, which was then washed with ethanol and acetone to yield a pure white precipitate.

**Fig. 3** ROS analysis using flow-cytometry technique showed: **A** untreated cells. **B** Cells treated with compound **5i**. **C** Cells treated with compound **5l**



#### 4.1.3 3-(4-Hydroxybenzylidene)-1-(p-tolyl)pyrrolidine-2,5-dione (**5a**)

Yield 78%; White solid; M.P. 286–288 °C;  $^1\text{H-NMR}$  (500 MHz,  $\text{DMSO-d}_6$ )  $\delta$  10.11 (s, 1H, OH), 7.54 (d,  $J=8.0$  Hz, 2H-Ar), 7.47 (br. s, 1H, CH), 7.30 (d,  $J=8.0$  Hz, 2H-Ar), 7.21 (d,  $J=7.4$  Hz, 2H-Ar), 6.88 (d,  $J=7.7$  Hz, 2H-Ar), 3.76 (s, 2H,  $\text{CH}_2$ ), 2.36 (s, 3H,  $\text{CH}_3$ );  $^{13}\text{C-NMR}$  (125 MHz,  $\text{DMSO-d}_6$ )  $\delta$  174.13, 170.78, 159.86, 138.10, 133.50, 132.99, 130.57, 129.74, 127.39, 125.75, 121.53, 116.46, 34.53, 21.23; **IR** (KBr,  $\text{cm}^{-1}$ ): 3342 (OH), 3055 (CH-Arom.), 2927 (CH-Aliph.), 1766 (C=O Asym.), 1691 (C=O Sym.), 1639 (C=C Aliph.), 1597, 1516 (C=C Arom.), 1400 (C-N), 1278 (C-O); **MS** ( $m/z$ ): 293 [ $\text{M}^+$ ].

#### 4.1.4 3-(3-Hydroxybenzylidene)-1-(p-tolyl)pyrrolidine-2,5-dione (**5b**)

Yield 74%; White solid; M.P. 272–274 °C;  $^1\text{H-NMR}$  (500 MHz,  $\text{DMSO-d}_6$ )  $\delta$  9.70 (s, 1H, OH), 7.46 (t,  $J=2.4$  Hz, 1H, CH), 7.35–7.28 (m, 3H-Ar), 7.23 (d,  $J=8.2$  Hz, 2H-Ar), 7.12 (d,  $J=7.7$  Hz, 1H-Ar), 7.07 (t,  $J=2.0$  Hz, 1H-Ar), 6.88 (dd,  $J=8.0, 2.3$  Hz, 1H-Ar), 3.79 (d,  $J=2.4$  Hz, 2H), 2.37 (s, 3H);  $^{13}\text{C-NMR}$  (125 MHz,  $\text{DMSO-d}_6$ )  $\delta$  173.95, 170.53, 158.15, 138.23, 135.79, 133.23, 130.55, 130.46, 129.78, 127.37, 125.55, 121.94, 117.61, 117.00, 34.65, 21.24; **IR** (KBr,  $\text{cm}^{-1}$ ): 3398 (OH), 3057 (CH-Arom.), 2939 (CH-Aliph.), 1757 (C=O Asym.),

1699 (C=O Sym.), 1649 (C=C Aliph.), 1597, 1514 (C=C Arom.), 1384 (C-N), 1280 (C-O); **MS** ( $m/z$ ): 293 [ $\text{M}^+$ ].

#### 4.1.5 3-(2-Hydroxybenzylidene)-1-(p-tolyl)pyrrolidine-2,5-dione (**5c**)

Yield 71%; White solid; M.P. 276–279 °C;  $^1\text{H-NMR}$  (500 MHz,  $\text{DMSO-d}_6$ )  $\delta$  10.29 (s, 1H, OH), 7.91 (t,  $J=2.4$  Hz, 1H, CH), 7.56 (dd,  $J=7.9, 1.6$  Hz, 1H-Ar), 7.33–7.23 (m, 5H-Ar), 7.01–6.89 (m, 2H-Ar), 3.79 (d,  $J=2.4$  Hz, 2H), 2.37 (s, 3H);  $^{13}\text{C-NMR}$  (125 MHz,  $\text{DMSO-d}_6$ )  $\delta$  174.15, 170.73, 157.62, 138.16, 131.98, 130.53, 129.76, 129.66, 127.86, 127.39, 123.88, 121.51, 119.95, 116.36, 34.47, 21.24; **IR** (KBr,  $\text{cm}^{-1}$ ): 3325 (OH), 3072 (CH-Arom.), 2926 (CH-Aliph.), 1757 (C=O Asym.), 1697 (C=O Sym.), 1645 (C=C Aliph.), 1598, 1516 (C=C Arom.), 1394 (C-N), 1246 (C-O); **MS** ( $m/z$ ): 293 [ $\text{M}^+$ ].

#### 4.1.6 3-(4-Hydroxy-3-methoxybenzylidene)-1-(p-tolyl)pyrrolidine-2,5-dione (**5d**)

Yield 85%; White solid; M.P. 226–228 °C;  $^1\text{H-NMR}$  (500 MHz,  $\text{DMSO-d}_6$ )  $\delta$  9.77 (s, 1H, OH), 7.49 (t,  $J=2.3$  Hz, 1H, CH), 7.31 (d,  $J=8.1$  Hz, 2H), 7.24–7.21 (m, 3H-Ar), 7.17 (dd,  $J=8.3, 2.0$  Hz, 1H-Ar), 6.90 (d,  $J=8.2$  Hz, 1H-Ar), 3.86 (s, 3H,  $\text{OCH}_3$ ), 3.83 (d,  $J=2.3$  Hz, 2H), 2.37 (s, 3H,  $\text{CH}_3$ );  $^{13}\text{C-NMR}$  (125 MHz,  $\text{DMSO-d}_6$ )  $\delta$  174.17, 170.76, 149.38, 148.25, 138.10, 133.87, 130.56,



129.73, 127.39, 126.16, 125.07, 121.65, 116.36, 114.52, 56.09, 34.42, 21.23; **IR** (KBr,  $\text{cm}^{-1}$ ): 3377 (OH), 3053 (CH-Arom.), 2902 (CH-Aliph.), 1757 (C=O Asym.), 1695 (C=O Sym.), 1649 (C=C Aliph.), 1593, 1516 (C=C Arom.), 1413 (C-N), 1294 (C-O); **MS** (m/z): 323 [ $\text{M}^+$ ].

#### 4.1.7 1-(4-Chlorophenyl)-3-(4-Hydroxybenzylidene)pyrrolidine-2,5-dione (5e)

Yield 76%; White solid; M.P. 282–284 °C;  **$^1\text{H-NMR}$**  (500 MHz,  $\text{DMSO-d}_6$ ):  $\delta$  10.17 (s, 1H, OH), 7.57 (dd,  $J=13.8, 8.5$  Hz, 4H-Ar), 7.49 (t,  $J=2.3$  Hz, 1H, CH), 7.41 (d,  $J=8.4$  Hz, 2H-Ar), 6.90 (d,  $J=8.2$  Hz, 2H-Ar), 3.77 (d,  $J=2.5$  Hz, 2H);  **$^{13}\text{C-NMR}$**  (125 MHz,  $\text{DMSO-d}_6$ ):  $\delta$  173.88, 170.47, 159.95, 133.82, 133.05, 132.04, 129.34, 129.31, 125.68, 121.30, 116.49, 34.60; **IR** (KBr,  $\text{cm}^{-1}$ ): 3400 (OH), 3062 (CH-Arom.), 2947 (CH-Aliph.), 1766 (C=O Asym.), 1695 (C=O Sym.), 1637 (C=C Aliph.), 1597, 1494 (C=C Arom.), 1388 (C-N), 1276 (C-O); **MS** (m/z): 313 [ $\text{M}^+$ ,  $^{35}\text{Cl}$ ].

#### 4.1.8 1-(4-Chlorophenyl)-3-(3-Hydroxybenzylidene)pyrrolidine-2,5-dione (5f)

Yield 64%; White solid; M.P. 248–250 °C;  **$^1\text{H-NMR}$**  (500 MHz,  $\text{DMSO-d}_6$ ):  $\delta$  9.70 (s, 1H, OH), 7.62–7.59 (m, 2H-Ar), 7.48 (t,  $J=2.4$  Hz, 1H, CH), 7.42–7.40 (m, 2H-Ar), 7.31 (t,  $J=7.9$  Hz, 1H-Ar), 7.13 (d,  $J=7.7$  Hz, 1H-Ar), 7.07 (t,  $J=2.0$  Hz, 1H-Ar), 6.88 (dd,  $J=8.0, 2.4$  Hz, 1H-Ar), 3.79 (d,  $J=2.4$  Hz, 2H);  **$^{13}\text{C-NMR}$**  (125 MHz,  $\text{DMSO-d}_6$ ):  $\delta$  173.71, 170.24, 158.16, 135.72, 133.51, 133.17, 131.93, 130.57, 129.38, 129.36, 125.39, 121.95, 117.69, 117.04, 34.73; **IR** (KBr,  $\text{cm}^{-1}$ ): 3419 (OH), 3097 (CH-Arom.), 2939 (CH-Aliph.), 1759 (C=O Asym.), 1703 (C=O Sym.), 1647 (C=C Aliph.), 1597, 1492 (C=C Arom.), 1382 (C-N), 1280 (C-O); **MS** (m/z): 313 [ $\text{M}^+$ ,  $^{35}\text{Cl}$ ].

#### 4.1.9 1-(4-Chlorophenyl)-3-(2-Hydroxybenzylidene)pyrrolidine-2,5-dione (5g)

Yield 68%; White solid; M.P. 266–268 °C;  **$^1\text{H-NMR}$**  (500 MHz,  $\text{DMSO-d}_6$ ):  $\delta$  10.30 (s, 1H, OH), 7.92 (t,  $J=2.4$  Hz, 1H, CH), 7.61–7.55 (m, 3H-Ar), 7.44–7.41 (m, 2H-Ar), 7.31–7.27 (m, 1H-Ar), 7.98–6.90 (m, 2H-Ar), 3.80 (d,  $J=2.4$  Hz, 2H);  **$^{13}\text{C-NMR}$**  (125 MHz,  $\text{DMSO-d}_6$ ):  $\delta$  173.91, 170.44, 157.66, 133.11, 132.08, 132.00, 129.67, 129.37, 129.34, 128.14, 123.69, 121.43, 119.97, 116.38, 34.55; **IR** (KBr,  $\text{cm}^{-1}$ ): 3327 (OH), 3099 (CH-Arom.), 2945 (CH-Aliph.), 1759 (C=O Asym.), 1701 (C=O Sym.), 1645 (C=C Aliph.), 1600, 1494 (C=C Arom.), 1388 (C-N), 1246 (C-O); **MS** (m/z): 313 [ $\text{M}^+$ ,  $^{35}\text{Cl}$ ].

#### 4.1.10 1-(4-Chlorophenyl)-3-(4-Hydroxy-3-methoxybenzylidene)pyrrolidine-2,5-dione (5h)

Yield 80%; White solid; M.P. 208–210 °C;  **$^1\text{H-NMR}$**  (500 MHz,  $\text{DMSO-d}_6$ ):  $\delta$  9.78 (s, 1H, OH), 7.63–7.58 (m, 2H-Ar), 7.50 (t,  $J=2.3$  Hz, 1H, CH), 7.45–7.39 (m, 2H-Ar), 7.23 (d,  $J=2.0$  Hz, 1H-Ar), 7.17 (dd,  $J=8.4, 2.0$  Hz, 1H-Ar), 6.90 (d,  $J=8.2$  Hz, 1H-Ar), 3.86 (s, 3H,  $\text{CH}_3\text{O}$ ), 3.83 (d,  $J=2.3$  Hz, 2H);  **$^{13}\text{C-NMR}$**  (125 MHz,  $\text{DMSO-d}_6$ ):  $\delta$  173.93, 170.46, 149.47, 148.26, 134.17, 133.04, 132.04, 129.36, 129.31, 126.09, 125.14, 121.44, 116.37, 114.55, 56.10, 34.49; **IR** (KBr,  $\text{cm}^{-1}$ ): 3375 (OH), 3186 (CH-Arom.), 2974 (CH-Aliph.), 1766 (C=O Asym.), 1705 (C=O Sym.), 1645 (C=C Aliph.), 1591, 1514 (C=C Arom.), 1388 (C-N), 1290 (C-O); **MS** (m/z): 343 [ $\text{M}^+$ ,  $^{35}\text{Cl}$ ].

#### 4.1.11 1-(4-Bromophenyl)-3-(4-Hydroxybenzylidene)pyrrolidine-2,5-dione (5i)

Yield 40%; White solid; M.P. 270–272 °C;  **$^1\text{H-NMR}$**  (500 MHz,  $\text{DMSO-d}_6$ ):  $\delta$  10.17 (s, 1H, OH), 7.74–7.71 (m, 2H-Ar), 7.55 (d,  $J=10$  Hz, 2H-Ar), 7.49 (t,  $J=5$  Hz, 1H, CH), 7.35–7.33 (m, 2H-Ar), 6.90 (d,  $J=8.3$  Hz, 2H-Ar), 3.76 (d,  $J=2.3$  Hz, 2H);  **$^{13}\text{C-NMR}$**  (125 MHz,  $\text{DMSO-d}_6$ ):  $\delta$  173.83, 170.41, 159.96, 133.84, 133.06, 132.47, 132.26, 129.63, 125.68, 121.54, 121.29, 116.49, 34.61; **IR** (KBr,  $\text{cm}^{-1}$ ): 3363 (OH), 3095 (CH-Arom.), 2947 (CH-Aliph.), 1766 (C=O Asym.), 1691 (C=O Sym.), 1637 (C=C Aliph.), 1597, 1490 (C=C Arom.), 1394 (C-N), 1278 (C-O); **MS** (m/z): 359 [ $\text{M}^+$ ,  $^{81}\text{Br}$ ].

#### 4.1.12 1-(4-Bromophenyl)-3-(3-Hydroxybenzylidene)pyrrolidine-2,5-dione (5j)

Yield 72%; White solid; M.P. 260–262 °C;  **$^1\text{H-NMR}$**  (500 MHz,  $\text{DMSO-d}_6$ ):  $\delta$  9.70 (s, 1H, OH), 7.75–7.73 (m, 2H-Ar), 7.48 (t,  $J=2.4$  Hz, 1H, CH), 7.37–7.29 (m, 3H-Ar), 7.13 (d,  $J=7.7$  Hz, 1H-Ar), 7.07 (t,  $J=1.9$  Hz, 1H-Ar), 6.88 (dd,  $J=8.0, 2.3$  Hz, 1H-Ar), 3.79 (d,  $J=2.5$  Hz, 2H);  **$^{13}\text{C-NMR}$**  (125 MHz,  $\text{DMSO-d}_6$ ):  $\delta$  173.66, 170.20, 158.16, 135.72, 133.52, 132.37, 132.33, 130.58, 129.66, 125.39, 121.96, 121.68, 117.69, 117.04, 34.73; **IR** (KBr,  $\text{cm}^{-1}$ ): 3390 (OH), 3093 (CH-Arom.), 2941 (CH-Aliph.), 1755 (C=O Asym.), 1699 (C=O Sym.), 1647 (C=C Aliph.), 1595, 1490 (C=C Arom.), 1400 (C-N), 1282 (C-O); **MS** (m/z): 357 [ $\text{M}^+$ ,  $^{81}\text{Br}$ ].

#### 4.1.13 1-(4-Bromophenyl)-3-(2-Hydroxybenzylidene)pyrrolidine-2,5-dione (5k)

Yield 85%; White solid; M.P. 268–271 °C;  **$^1\text{H-NMR}$**  (500 MHz,  $\text{DMSO-d}_6$ ):  $\delta$  10.31 (s, 1H, OH), 7.93 (t,  $J=5$  Hz, 1H, CH), 7.75–7.71 (m, 2H-Ar), 7.56 (dd,  $J=8.0$ ,

1.7 Hz, 1H-Ar), 7.37–7.27 (m, 3H-Ar), 7.01–6.88 (m, 2H-Ar), 3.79 (d,  $J = 2.4$  Hz, 2H);  $^{13}\text{C-NMR}$  (125 MHz, DMSO- $d_6$ ):  $\delta$  173.86, 170.38, 157.66, 132.43, 132.29, 132.08, 129.66, 128.16, 123.68, 121.61, 121.43, 119.97, 116.38, 34.56; **IR** (KBr,  $\text{cm}^{-1}$ ): 3338 (OH), 3097 (CH-Arom.), 2943 (CH-Aliph.), 1757 (C=O Asym.), 1701 (C=O Sym.), 1645 (C=C Aliph.), 1598, 1492 (C=C Arom.), 1400 (C–N), 1246 (C–O); **MS** ( $m/z$ ): 357 [ $\text{M}^+$ ,  $^{81}\text{Br}$ ].

#### 4.1.14 1-(4-Bromophenyl)-3-(4-Hydroxy-3-methoxybenzylidene)pyrrolidine-2,5-dione (5l)

Yield 83%; White solid; M.P. 238–240 °C;  $^1\text{H-NMR}$  (500 MHz, DMSO- $d_6$ )  $\delta$  9.73 (s, 1H, OH), 7.74–7.71 (m, 2H-Ar), 7.50 (t,  $J = 5$  Hz, 1H, CH), 7.36–7.33 (m, 2H-Ar), 7.23 (s, 1H-Ar), 7.16 (d,  $J = 10.2$  Hz, 1H-Ar), 6.88 (d,  $J = 8.2$  Hz, 1H-Ar), 3.85 (s, 3H,  $\text{CH}_3\text{O}$ ), 3.83 (s, 2H);  $^{13}\text{C-NMR}$  (125 MHz, DMSO- $d_6$ ):  $\delta$  172.8, 169.33, 148.39, 147.17, 133.09, 131.28, 128.58, 124.05, 120.40, 115.29, 113.45, 55.01, 33.41; **IR** (KBr,  $\text{cm}^{-1}$ ): 3375 (OH), 3064 (CH-Arom.), 2939 (CH-Aliph.), 1764 (C=O Asym.), 1705 (C=O Sym.), 1643 (C=C Aliph.), 1589, 1514 (C=C Arom.), 1384 (C–N), 1263 (C–O); **MS** ( $m/z$ ): 389 [ $\text{M}^+$ ,  $^{81}\text{Br}$ ].

## 4.2 Biological Evaluation Section

### 4.2.1 Evaluation of Antimicrobial Activities

The broth micro-dilution method was used to determine the minimum inhibitory concentrations; MICs values, which are defined by CLSI (Clinical Laboratory Standard Institute) as the lowest concentration of each assessed compound required to inhibit visible growth of the tested bacterium. In brief, two-fold serial dilutions of each compound were made in sterile micro-dilution trays containing Mueller Hinton broth medium at concentrations ranging from 0.003 to 4  $\mu\text{g/ml}$ . Then, in sterile normal saline adjusted to 0.5 McFarland standard turbidity, bacterial suspensions of each bacterial strain were prepared from freshly cultured cells. Just before adding the suspension to the trays containing a serial dilution of each compound, the suspension was further diluted (1:100) with sterile Mueller–Hinton broth (MHB). As a result, each compound concentration was tested against  $0.5\text{--}1 \times 10^6$  microbial cells. For 24 h, 96 well plates were incubated at 37 °C, as a growth indicator, resazurin was used. In brief, 4  $\mu\text{L}$  of 4 mg/ml reagent stock solution in sterile distilled water were added to each well. While pinkish wells indicate bacterial growth, any blue well indicates inhibition of growth by the tested compound. Cefixime was evaluated as a standard antibiotic against bacterial strains, while cycloheximide was evaluated as a standard antifungal compound. All experiments were carried out in triplicate [36, 37].

### 4.2.2 Evaluation of Anticancer Activity

The National Cell Bank of Iran provided MCF-7 (a human breast cancer cell line) (Pasteur Institute, Iran). Cells were cultured in RPMI-1640 (Gibco) and DMEM medium (Gibco) with 10% FBS (Gibco) and antibiotics (100 U/ml penicillin and 100  $\mu\text{g/ml}$  streptomycin). Cells were cultured at 37 °C in humidified air with 5%  $\text{CO}_2$  and passaged with trypsin/EDTA (Gibco) and phosphate-buffered saline (PBS) solution. The culturing media and conditions used to grow the cells as 3D colonies were identical to those used for monolayer cell culture.

### 4.3 Cell Viability Assay

The MTT [3-(4, 5-dimethylthiazol-2-yl)-2, 5-diphenyltetrazolium Bromide] assay was used to measure cell growth and viability. In brief, cells were digested with trypsin, harvested, adjusted to a density of  $1.4 \times 10^4$  cells/well, and seeded for 24 h in 96-well plates filled with 200  $\mu\text{L}$  fresh medium per well. When the cells formed a monolayer, they were treated for 24 h at 37 °C in 5%  $\text{CO}_2$  with 100–6.25  $\mu\text{g/ml}$  of the compounds, involved cis-platin as positive control. At the end of the treatment (24 h), the supernatant was removed and 200  $\mu\text{l/well}$  of MTT solution (0.5 mg/ml in phosphate-buffered saline [PBS]) was added to the plate, which was then incubated at 37 °C for an additional 4 h. MTT solution (the supernatant of cells was removed and dimethyl sulfoxide (100  $\mu\text{l}$  per well) was added. Cells were shaken at 37 °C until the crystals were completely dissolved. The absorbance at 570 nm was measured with an ELISA reader to determine cell viability (Model wave xs2, BioTek, USA). The concentration of the compounds that caused 50% cell death ( $\text{IC}_{50}$ ) was calculated using dose–response curves [38].

### 4.4 Fluorescent Staining

The Ethidium bromide/acridine orange (EB/AO) stain was used to determine cellular viability (Live/Dead). MCF7 cells were seeded in 6 well cell culture plates and treated for 24 h with the  $\text{IC}_{50}$  concentration of the compounds. After washing the cells with PBS, a solution containing EB/AO was added, and the stained cells were immediately visualized and imaged using a fluorescence microscope (Axioskop 2 plus, Zeiss, Germany) [39].

### 4.5 Apoptosis Assay

The Annexin V-FITC apoptosis kit was used to identify apoptotic and necrotic MCF-7 cells treated with 5i and 5l compounds (BioVision). After 4 h of treatment with the  $\text{IC}_{50}$  concentrations of 5i and 5l (31.4 and 52.6  $\mu\text{g/ml}$ ,

respectively), cells were harvested, thoroughly washed, and labeled with PI and FITC according to the kit manufacturer's protocol. In brief,  $5 \times 10^5$  cells were harvested and centrifuged after being treated with **5i** and **5I**  $IC_{50}$  values for 24 h, as well as untreated control cells for 10 min. The pellet was then re-suspended in 500 l  $\times$  binding buffer, 5  $\mu$ l annexin V-FITC, and 5  $\mu$ l propidium iodide (50  $\mu$ g/ml) were added, and incubated at room temperature for 5 min. Following incubation, the stained cells were analyzed using a FACS analysis machine (flow cytometry apparatus, Partec PAS, Germany). The distribution of differentially labeled cells was determined by collecting signals from annexin V-FITC labeled cells using a FITC signal detector (FL1) and PI stained cells using a FL3 signal detector [40].

#### 4.6 Reactive Oxygen Species Assay

Flow cytometry was used to measure ROS production using 2',7'-dichlorodihydrofluorescein diacetate (DCFH2-DA) (Sigma-Aldrich). This dye enters cells easily and is hydrolyzed by intracellular esterase to produce 2',7' dichlorodihydrofluorescein (DCFH2), which is trapped within the cells. DCFH2 is oxidized by hydrogen peroxide or low molecular weight peroxides produced by the cells to the highly fluorescent compound 2',7'-dichlorofluorescein (DCF). As a result, the intensity of the fluorescence was proportional to the amount of hydrogen peroxide produced by the cells. MCF7 ( $1 \times 10^5$  cells/well) cells were treated for 12 h with the  $IC_{50}$  concentration of the compounds. Thirty minutes before the end of the experiment, cells were trypsinized, centrifuged for 5 min, and the pellet washed with 1 mL of PBS before being treated with DCFH2-DA and stored in the dark. After 30 min, the fluorescence was evaluated by comparing two fluorescence excitation/emission 485–495 nm and 525–530 nm [41].

**Supplementary Information** The online version contains supplementary material available at <https://doi.org/10.1007/s42250-023-00710-7>.

**Acknowledgements** This research project is funded by the Ministry of Higher Education and Scientific Researches, University of Basrah, College of Education for Pure Sciences, Department of Chemistry, Iraq, and is part of the master program's graduation requirements. The authors would like to thank Tehran Central Laboratory, University of Tehran, Iran for their help in characterization techniques and biological tests.

**Data availability** Not applicable.

#### Declarations

**Conflict of interest** The authors declare there is no conflict of interest.

**Ethical approval** Not applicable.

**Informed consent** Informed consent was obtained from all individual participants included in the study.

#### References

- Vidović D, Milošević N, Pavlović N, Todorović N, Panić JČ, Čurčić J et al (2022) In silico-in vitro estimation of lipophilicity and permeability association for succinimide derivatives using chromatographic anisotropic systems and parallel artificial membrane permeability assay. *Biomed Chromatogr* 36(9):e5413. <https://doi.org/10.1002/bmc.5413>
- Hassan ZF, Shirini F, Mamaghani M, Daneshvar N (2021) Introduction of succinimide as a green and sustainable organocatalyst for the synthesis of arylidene malononitrile and tetrahydrobenzo[b]pyran derivatives. *Comb Chem High Throughput Screen* 24(1):155–163. <https://doi.org/10.2174/1386207323666200709170916>
- Ravasco JM, Faustino H, Trindade A, Gois PM (2019) Bioconjugation with maleimides: a useful tool for chemical biology. *Chem Eur J* 25:43–59
- Zhang Q, Wang J, Yang S, Cheng J, Ding G, Huo S (2019) Facile construction of one-component intrinsic flame-retardant epoxy resin system with fast curing ability using imidazole-blocked bis-maleimide. *Compos Part B Eng* 177:107380. <https://doi.org/10.1016/j.compositesb.2019.107380>
- Mhaske SB, Argade NP (2003) Base-induced alcoholysis of N-arylmaleimides: facile in situ Oxa-Michael addition to alkyl maleanilates: two-step one-pot rapid access to alkoxy-succinic acids. *Synthesis* 6:0863–0870. <https://doi.org/10.1055/s-2003-38693>
- Chauhan P, Kaur J, Chimni SS (2013) Asymmetric organocatalytic addition reactions of maleimides: a promising approach towards the synthesis of chiral succinimide derivatives. *Chem Asian J* 8(2):328–346. <https://doi.org/10.1002/asia.201200684>
- Dua R, Shrivastava S, Sonwane SK, Srivastava SK (2011) Pharmacological significance of synthetic heterocycles scaffold: a review. *Adv Biol Res* 5(3):120–144
- Fredenhagen A, Tamura Y, Kenny T, Komura H, Naya Y, Nakaniishi K et al (1987) Andrimid, a new peptide antibiotic produced by an intracellular bacterial symbiont isolated from a brown planthopper. *J Am Chem Soc* 109:4409
- Corrêa R, Filho VC, Rosa PW, Pereira CI, Schlemper V, Nunes RJ (1997) Synthesis of new succinimides and sulphonated derivatives with analgesic action in mice. *Pharma Pharmacol Commun* 3:67–71
- Hall IH, Wong OT, Scovill JP (1995) The cytotoxicity of N-pyridinyl and N-quinolinyl substituted derivatives of phthalimide and succinimide. *Biomed Pharmacother* 49:251–258
- Filho VC, Nunes RJ, Calixto JB, Yunes RA (1995) Inhibition of guinea-pig ileum contraction by phyllanthimide analogues: structure-activity relationships. *Pharma Pharmacol Commun* 1:399–401
- Zentz F, Valla A, Le Guillou R, Labia R, Mathot AG, Sirot D (2002) Synthesis and antimicrobial activities of N-substituted imides. *Farmaco* 57(5):421–426. [https://doi.org/10.1016/S0014-827X\(02\)01217-X](https://doi.org/10.1016/S0014-827X(02)01217-X)
- Hazra B, Pore V, Dey S, Datta S, Darokar M, Saikia D et al (2004) Bile acid amides derived from chiral amino alcohols: novel antimicrobials and antifungals. *Bioorg Med Chem Lett* 14(3):773–777. <https://doi.org/10.1016/j.bmcl.2003.11.018>
- Zhao Z, Yue J, Ji X, Nian M, Kang K, Qiao H et al (2021) Research progress in biological activities of succinimide

- derivatives. *Bioorg Chem* 108:104557. <https://doi.org/10.1016/j.bioorg.2020.104557>
15. Rosenqvist P, Mäkinen JJ, Palmu K, Jokinen J, Prajapati RK, Korhonen HJ et al (2022) The role of the maleimide ring system on the structure-activity relationship of showdomycin. *Eur J Med Chem* 237:114342. <https://doi.org/10.1016/j.ejmech.2022.114342>
  16. Lopes-Ortiz MA, Panice MR, de Melo EB, Ataíde Martins JP, Baldin VP, Agostinho Pires CT et al (2020) Synthesis and anti-*Mycobacterium tuberculosis* activity of imide- $\beta$ -carboline and carbomethoxy- $\beta$ -carboline derivatives. *Eur J Med Chem* 187:111935. <https://doi.org/10.1016/j.ejmech.2019.111935>
  17. Cieślak M, Napiórkowska M, Kaźmierczak-Barańska J, Królewska-Golińska K, Hawrył A, Wybrańska I et al (2021) New succinimides with potent anticancer activity: synthesis, activation of stress signaling pathways and characterization of apoptosis in leukemia and cervical cancer cells. *Int J Mol Sci* 22(9):4318. <https://doi.org/10.3390/ijms22094318>
  18. Hashim HT, Ramadhan MA, Theban KM, Bchara J, El-Abed-El-Rassoul A, Shah J (2021) Assessment of breast cancer risk among Iraqi women in 2019. *BMC Womens Health* 21(1):412. <https://doi.org/10.1186/s12905-021-01557-1>
  19. Al-Hashimi MMY (2021) Trends in breast cancer incidence in Iraq during the period 2000–2019. *Asian Pac J Cancer Prev* 22(12):3889–3896. <https://doi.org/10.31557/APJCP.2021.22.12.3889>
  20. Finiuk N, Kryshchshyn-Dylevych A, Holota S, Klyuchivska O, Kozyskiy A, Karpenko O et al (2022) Novel hybrid pyrrolidin-2-one-thiazolidinones as potential anticancer agents: Synthesis and biological evaluation. *Eur J Med Chem* 238:114422. <https://doi.org/10.1016/j.ejmech.2022.114422>
  21. Xue Z, Xiao L, Chen H, Zhou T, Qian Y, Suo J et al (2018) Synthesis and evaluation of a novel “off-on” chemical sensor based on rhodamine B and the 2,5-pyrrolidinedione moiety for selective discrimination of glutathione and its bioimaging in living cells. *Bioorg Med Chem* 26(8):1823–1831. <https://doi.org/10.1016/j.bmc.2018.02.030>
  22. Milosevic NP, Kojic V, Curcic J, Jakimov D, Milic N, Banjac N et al (2017) Evaluation of in silico pharmacokinetic properties and in vitro cytotoxic activity of selected newly synthesized N-succinimide derivatives. *J Pharm Biomed Anal* 137:252–257. <https://doi.org/10.1016/j.jpba.2017.01.042>
  23. Liu T, Song S, Wang X, Hao J (2021) Small-molecule inhibitors of breast cancer-related targets: potential therapeutic agents for breast cancer. *Eur J Med Chem* 210:112954. <https://doi.org/10.1016/j.ejmech.2020.112954>
  24. Matuszak N, Muccioli GG, Labar G, Lambert DM (2009) Synthesis and in vitro evaluation of N-substituted maleimide derivatives as selective monoglyceride lipase inhibitors. *J Med Chem* 52(23):7410–7420. <https://doi.org/10.1021/jm900461w>
  25. Kalia D, Malekar PV, Parthasarathy M (2016) Exocyclic olefinic maleimides: synthesis and application for stable and thiol-selective bioconjugation. *Angew Chem Int Ed Engl* 55(4):1432–1435. <https://doi.org/10.1002/anie.201508118>
  26. Xia L, Zhai X, Xiong X, Chen P (2014) Synthesis and properties of 1, 3, 4-oxadiazole-containing bismaleimides with asymmetric structure and the copolymerized systems thereof with 4, 4'-bismaleimidodiphenylmethane. *RSC Adv* 4:4646–4655
  27. Abushaheen MA, Fatani AJ, Alosaimi M, Mansy W, George M, Acharya S et al (2020) Antimicrobial resistance, mechanisms and its clinical significance. *Dis Mon* 66(6):100971. <https://doi.org/10.1016/j.disamonth.2020.100971>
  28. Fair RJ, Tor Y (2014) Antibiotics and bacterial resistance in the 21st century. *Perspect Medicin Chem* 6:25–64. <https://doi.org/10.4137/PMC.S14459>
  29. Clardy J, Fischbach MA, Currie CR (2009) The natural history of antibiotics. *Curr Biol* 19(11):R437–R441. <https://doi.org/10.1016/j.cub.2009.04.001>
  30. Lin J, Zhou D, Steitz TA, Polikanov YS, Gagnon MG (2018) Ribosome-targeting antibiotics: modes of action, mechanisms of resistance, and implications for drug design. *Annu Rev Biochem* 87:451–478. <https://doi.org/10.1146/annurev-biochem-062917-011942>
  31. Gil-Gil T, Laborda P, Sanz-García F, Hernando-Amado S, Blanco P, Martínez JL (2019) Antimicrobial resistance: a multifaceted problem with multipronged solutions. *Microbiolopen* 8(11):945. <https://doi.org/10.1002/mbo3.945>
  32. Ahmad A, Ullah F, Sadiq A, Ayaz M, Rahim H, Rashid U, Ahmad S, Jan MS, Ullah R, Shahat AA, Mahmood HM (2019) Pharmacological evaluation of aldehydic-pyrrolidinedione against HCT-116, MDA-MB231, NIH/3T3, MCF-7 cancer cell lines, antioxidant and enzyme inhibition studies. *Drug Des Dev Ther* 13:4185–4194. <https://doi.org/10.2147/DDDT.S226080>
  33. Zentz F, Valla A, Le Guillou R, Labia R, Mathot AG, Sirot D (2002) Synthesis and antimicrobial activities of N-substituted imides. *Farmaco* 57(5):421–426. [https://doi.org/10.1016/s0014-827x\(02\)01217-x](https://doi.org/10.1016/s0014-827x(02)01217-x)
  34. Zentz F, Le Guillou R, Labia R, Sirot D, Linard B, Valla A (2004) Syntheses, in vitro antibacterial and cytotoxic activities of a series of 3-substituted succinimides. *Farmaco* 59(11):879–886. <https://doi.org/10.1016/j.farmac.2004.07.007>
  35. Yang CP, Wang SS (1989) Studies on the imidization of N-substituted polymaleamic acids. *J Appl Polym Sci* 27(1):15–29. <https://doi.org/10.1002/pola.1989.080270102>
  36. AbdulJabar L, Mutalq D, Al-Shawi A (2021) Synthesis of novel 2-thioxo-4-imidazolidinone derivatives and evaluate their antibacterial and antifungal activities. *Egypt J Chem* 64(6):3059–3067. <https://doi.org/10.21608/ejchem.2021.66960.3442>
  37. Yousif Aala A, Al-Shawi AAA, Hameed MF (2021) Antioxidant, antibacterial, and anticancer properties of Haloxylon salicornicum extracted by microwave-assisted extraction. *Egypt Pharm J* 20(3):225–231. [https://doi.org/10.4103/epj.epj\\_23\\_21](https://doi.org/10.4103/epj.epj_23_21)
  38. Haddad B, Al-Shawi A (2020) Cytotoxicity of new selenoimine, selenonitrene and nitrene derivatives against human breast cancer MDA-MB231 cells. *Egypt J Chem* 63(11):4607–4613. <https://doi.org/10.21608/ejchem.2020.31747.2675>
  39. Hameed MF, Mkashaf IA, Al-Shawi AAA, Hussein KA (2021) Antioxidant and anticancer activities of heart components extracted from Iraqi *Phoneix Dactylifera* Chick. *Asian Pac J Cancer Prev* 22(11):3533–3541. <https://doi.org/10.31557/APJCP.2021.22.11.3533>
  40. AbdulJabar LA, Al-Shawi AA, Mutalq DZ (2021) Anti-liver and anti-breast cancer activities of 2-thioxo-4-imidazolidinone derivatives. *Med Chem Res* 30:1943–1953. <https://doi.org/10.1007/s00044-021-02769-8>
  41. Thawini HK, Al-Shawi AA (2021) Polysaccharide of *Ziziphos spina-Christi* L. and its silver nanoparticles induced reactive oxygen species and late apoptosis in liver cancer cells. *Nanomed Res J* 6(3):237–247. <https://doi.org/10.22034/NMRJ.2021.03.004>

Springer Nature or its licensor (e.g. a society or other partner) holds exclusive rights to this article under a publishing agreement with the author(s) or other rightsholder(s); author self-archiving of the accepted manuscript version of this article is solely governed by the terms of such publishing agreement and applicable law.